First Principles Molecular Dynamics Study of Ziegler–Natta Heterogeneous Catalysis

3 AUTHORS, INCLUDING:

Mauro Boero

Institut de Physique et Chimie des Matériaux …

187 PUBLICATIONS **3,472** CITATIONS

SEE PROFILE

K. Terakura

National Institute of Advanced Industrial Sci…

374 PUBLICATIONS **13,123** CITATIONS

SEE PROFILE

First Principles Molecular Dynamics Study of Ziegler−Natta Heterogeneous Catalysis

Mauro Boero,*,† Michele Parrinello,† and Kiyoyuki Terakura‡

*Contribution from the Max Planck Institut für Festkörperforschung,
Heisenbergstrasse 1, D-70569 Stuttgart, Germany, and Joint Research Center for Atom Technology
(JRCAT), National Institute for Advanced Interdisciplinary Research (NAIR),
1-1-4 Higashi, Tsukuba, Ibaraki 305, Japan*

Abstract: We present a first principles study of the Ziegler−Natta $MgCl_2$-supported polymerization of ethylene in the framework of the Car-Parrinello approach. In particular we investigate the titanium active sites on the (110) surface of the support focusing on Corradini's model and the possible alternative configurations. We find that different catalyst sites are allowed and that the relevant energetics as well as the reactivity in the alkyl chain formation process strongly depend on the local geometry. During deposition of $TiCl_4$ and complex formation, which are energetically downhill, the dynamical approach allows us to follow the reaction pathway in an unbiased way. By means of Car−Parrinello constrained molecular dynamics we then determine the free energy profiles and estimate activation barriers in the alkene insertion processes. Furthermore a dynamical study of the insertion of a second ethylene molecule offers an interesting insight into the chain growth process and the stereochemical character of the polymer, providing a complete picture of the reaction mechanism.

Introduction

The Ziegler−Natta polymerization of α-olefins is well-known as one of the most stereospecific catalysis processes. Since its discovery,[1,2] which dates back to the early 1950s, this class of catalytic reactions has gained an overwhelming importance in many industrial applications where production of polymers with a high degree of enantioselectivity is required.[3−6]

Despite its widespread use, a full understanding of the polymerization mechanisms is still far from complete. The short time scale of the reaction is very skillfully used to enhance production efficiency, but poses severe limitations on detailed experimental studies. Thus, most of the extensive results coming from experiments[7−14] turn out to be indirect to varying degrees. It is then of fundamental importance to investigate theoretically the various reaction steps with the aim of elucidat-

ing the reaction pathway and, in a longer term perspective, to suggest or address improvements in the efficiency of polyolefins production. In this attempt much theoretical[15−23] work has been aimed at depicting the mechanism of the reaction and the role of the catalyst.

In a standard preparation of magnesium chloride/titanium chloride system, the catalyst coordinates onto an active surface of the support.[14] A very good choice for the support is made by cleaving $MgCl_2$ to form a (110) plane. On this surface $TiCl_4$ can stick efficiently, giving a high density of active sites.[24,25]

As far as the reaction pathway is concerned, one of the most accredited models, although rather qualitative in its original formulation, is the Cossee−Arlman mechanism[26] where an incoming alkene coordinates to a vacant site of Ti via its carbon double bond. This picture assumes an undercoordinated transition metal, e.g. a 5-fold titanium site, in which one of the bonds is a Ti−C. The carbon atom bound to the metal can belong to

† Max-Planck-Institut für Festkörperforschung.

‡ JRCAT-NAIR.

(1) Ziegler, K.; Holzkamp, E.; Breil, H.; Martin, H. *Angew. Chem.* **1954**, *67*, 541.

(2) Natta, G. *Macromol. Chem.* **1955**, *16*, 213.

(3) Keii, T. *Kinetics of Ziegler−Natta Polymerization*; Kodansha: Tokyo, 1972.

(4) Boor, J., Jr. *Ziegler−Natta Catalysis and Polymerization*; Academic Press: New York, 1979.

(5) See, for example: *Ziegler Catalysts*; Fink, G., Mülhaupt, R., Brintziger, H. H., Eds.; Springer-Verlag: Heidelberg, 1994.

(6) Glichrist, J. H.; Bercaw, J. E. *J. Am. Chem. Soc.* **1996**, *118*, 12021.

(7) Chien, J. C. W.; Bres, P. L. *J. Polym. Sci. A* **1986**, *24*, 2483 and references therein.

(8) Soga, K.; Shiono, T.; Doi, Y. *Makromol. Chem.* **1988**, *189*, 1531.

(9) Terano, M.; Kataoka, T.; Keii, T. *J. Polym. Sci. A* **1990**, *28*, 2035.

(10) Jones, P. J. V.; Oldman, R. J. *Transition Metals and Organometallics as Catalysts for Olefin Polymerization*; Kaminsky, W., Sinn, H., Eds.; Springer-Verlag: Berlin, 1988; p 223.

(11) Magni, E.; Somorjai, G. A. *Catal. Lett.* **1995**, *35*, 205.

(12) Magni, E.; Somorjai, G. A. *Appl. Surf. Sci.* **1995**, *89*, 187.

(13) Magni, E.; Somorjai, G. A. *Surf. Sci.* **1996**, *345*, 1.

(14) See, for example: Somorjai, G. A. *Introduction to Surface Chemistry and Catalysis*; J. Wiley & Sons: New York, 1994.

(15) Giunchi, G.; Clementi, E.; Ruiz-Vizcaya, M. E.; Novaro, O. *Chem. Phys. Lett.* **1977**, *49*, 8.

(16) Novaro, O.; Blaisten-Barojas, E.; Clementi, E.; Giunchi, G.; Ruiz-Vizcaya, M. E. *J. Chem. Phys.* **1978**, *68*, 2337.

(17) Fujimoto, H.; Yamasaki, T.; Mizutani, H.; Koga, N. *J. Am. Chem. Soc.* **1985**, *107*, 6157.

(18) Jolly, C. A.; Marynick, D. S. *J. Am. Chem. Soc.* **1989**, *111*, 7968.

(19) Kawamura-Kuribayashi, H.; Koga, N.; Morokuma, K. *J. Am. Chem. Soc.* **1992**, *114*, 2359.

(20) Weiss, H.; Ehrig, M.; Ahlrichs, R. *J. Am. Chem. Soc.* **1994**, *116*, 4919.

(21) Colbourn, E. A.; Cox, P. A.; Carruthers, B.; Jones, P. J. V. *J. Mater. Chem.* **1994**, *4*, 805.

(22) Jensen, V. R.; Børve, K. J.; Ystenes M. *J. Am. Chem. Soc.* **1995**, *117*, 4109.

(23) Puhakka, E.; Pakkanen, T. T.; Pakkanen, T. A. *Surf. Sci.* **1995**, *334*, 289.

(24) Corradini, P.; Busico, V.; Guerra, G. Monoalkene Polymerization: Stereospecificity. In *Comprehensive Polymer Science* **1988**, *4*, 29−50.

(25) Busico, V.; Cipullo, R.; Corradini, P.; De Biasio, R. *Macromol. Chem. Phys.* **1995**, *196*, 491.

(26) Cossee, P. *J. Catal.* **1964**, *3*, 80. Arlman, E. *J. Catal.* **1964**, *3*, 89. Arlman, E.; Cossee, P. *J. Catal.* **1964**, *3*, 99.
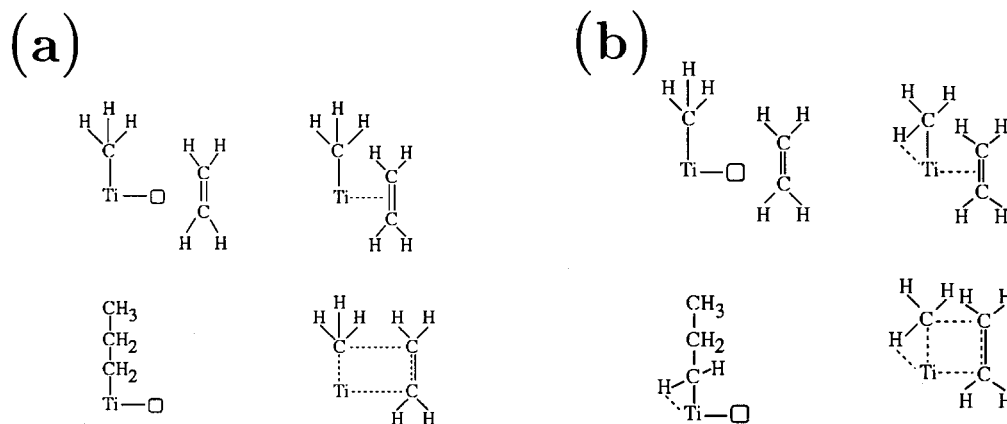
Figure 1. Possible reaction pathways for the ethylene insertion. The former (a) is the Cossee−Arlman mechanism, the latter (b) the Brookhart−Green one. (Both schemes are read clockwise starting from the upper left.)

a methyl group acting as chain-terminator as well as to a CH_2 unit of the already formed polymeric chain. The next steps consist of a transition state in which the Ti−C and the two doubly bound carbon atoms of the incoming molecule form a four-member ring structure and a final state in which the complete insertion occurs (Figure 1a).

A possible alternative to the Cossee−Arlman picture was proposed by Brookhart and Green.[27] In their scheme, the insertion of the olefin proceeds from a π-complex configuration similar to the Cossee−Arlman one but is assisted by an agostic interaction of the Ti and a nearby hydrogen belonging to the growing polymeric chain. This reduces steric repulsions between H atoms of the chain and those of the alkene (Figure 1b). Other more complicated mechanisms involving hydrogen migration processes such as the Green−Rooney scheme have been ruled out by isotope experiments.[28]

Although neither mechanism has yet been experimentally proven, several quantum chemical calculations and potential energy surface (PES) analysis have been performed in the attempt to clarify the various stages that lead to the first insertion.[15−22] For analogous homogeneous systems several investigations have been reported, but for the heterogeneous catalysis very little has been done and a general consensus has not yet been achieved.

In the present work we analyze the titanium active sites on a $MgCl_2$ (110) surface. In particular, we investigate the most accreditated configurations of Ti reported in refs 24 and 25 and in ref 23. Furthermore, we present a formation of a 5-fold titanium site in a very unbiased way, simulating the deposition of a $TiCl_4$ molecule onto the substrate. The energetics and reactivity of the various competing configurations are carefully investigated both statically and dynamically. Computer experiments of the insertion of ethylenes yield an interesting overview of the first step of the polymerization and the subsequent chain rearrangement and propagation as a response to further addition of olefins. The present calculations have thereby clarified the reaction mechanism and opened the way for dynamical simulations of realistic heterogeneous systems.

Computational Method

We performed ab initio molecular dynamics simulations using the Car−Parrinello scheme[29] (CPMD). Our approach is based on density functional theory within the local density approximation (LDA) on

exchange and correlation, using the Ceperley−Alder correlation functional[30] interpolated with the Perdew−Zunger formulas.[31] Our LDA results were checked by comparison with Becke−Lee−Yang−Parr[32,33] (BLYP) gradient-corrected functional calculations. Dynamical simulations were performed at BLYP level when not otherwise specified in the text.

Trouiller and Martins[34] norm-conserving pseudopotentials were used to account for the valence−core interactions, including nonlinear core corrections[35] for titanium, and wave functions were expanded in a plane wave basis set with an energy cutoff of 40 Ry. We checked the convergence of this choice by testing our pseudopotentials on several reference molecules and comparing our results with both experimental data and all-electron calculations.[36]

Our $MgCl_2$ substrate was a monoclinic supercell of $12.729 \times 11.782 \times 27.512$ Å³ ($\angle ab = 72°$) containing 24 formula units. This amounts to a thickness of six layers of $MgCl_2$; the large z dimension ensures a good simulation of the empty space above the surface, which is necessary to accommodate $TiCl_4$ adducts and olefins. Periodic images of the Ti active site in the x and y directions are separated from each other by 17.376 Å.

Constant temperature simulations were performed setting the temperature at the typical experimental value[7,9] of 323 K. Since the reaction path involved overcoming relatively large activation barriers, the so-called "Blue Moon" ensemble method of refs 38−44 was adopted. Thus we performed constrained dynamics adding an holonomic constraint

(30) Ceperley, D. M.; Alder, B. J. *Phys. Rev. Lett.* **1980**, *45*, 566.

(31) Perdew, J. P.; Zunger, A. *Phys. Rev. B* **1981**, *23*, 5048.

(32) Becke, A. D. *Phys. Rev. A* **1988**, *38*, 3098.

(33) Lee, C.; Yang, W.; Parr, R. G. *Phys. Rev. B* **1988**, *37*, 785.

(34) Trouiller, N.; Martins, J. L. *Phys. Rev. B* **1991**, *43*, 1993.

(35) Louie, S. G.; Froyen S.; Cohen M. L. *Phys. Rev. B* **1982**, *26*, 1738.

(36) Tests have been performed on $MgCl_2$, MgO, $TiCl_4$, and TiO_2 molecules. Experimental data were taken from ref 52. All-electron calculations were done by Horst Weiss with the triple-ζ valence polarization (TZVP) basis set within the same LDA and BLYP functionals using TURBOMOLE.[37] Pseudopotentials results concerning the equilibrium geometries were in very good agreement with both all-electron findings (<0.3%) and reported measurements.

(37) (a) Ahlrichs, R.; Bär, M.; Häser, M.; Horn, H.; Kölmel, C. *Chem. Phys. Lett.* **1989**, *162*, 165. (b) Ahlrichs, R.; v. Arnim, M. TURBOMOLE, Parallel Implementation of SCF, Density Functional, and Chemical Shift Modules. In *Methods and Techniques in Computational Chemistry: METECC-95*; Clementi, E., Corongiu, G., Eds.; 1995.

(38) Ryckaert; J. P.; Ciccotti, G. *J. Chem. Phys.* **1983**, *78*, 7368.

(39) Ciccotti, G.; Ferrario, M.; Hynes, J. T.; Kapral, R. *Chem. Phys.* **1989**, *129*, 241.

(40) Carter, E. A.; Ciccotti, G.; Hynes, J. T.; Kapral, R. *Chem. Phys. Lett.* **1989**, *156*, 472.

(41) Paci, E.; Ciccotti, G.; Ferrario, M.; R. Kapral, R. *Chem. Phys. Lett.* **1991**, *176*, 581.

(42) Ciccotti, G.; Ferrario, M. In *Monte Carlo and Molecular Dynamics of Condensed Matter Systems*, *Proc. of Euroconference on Computer Simulation in Condensed Matter Physics and Chemistry*; Binder, K., Ciccotti, G., Eds.; SIF: Como, 1995.

(43) Straatsma, T. P.; Zacharias, M.; McCammon, J. A. *Chem. Phys. Lett.* **1992**, *196*, 297.

(27) Brookhart, M.; Green, M. L. H. *J. Organomet. Chem.* **1983**, *250*, 395.

(28) Soto, J.; Steigerwald, M. L.; Grubbs, R. H. *J. Am. Chem. Soc.* **1982**, *104*, 4479 and references therein.

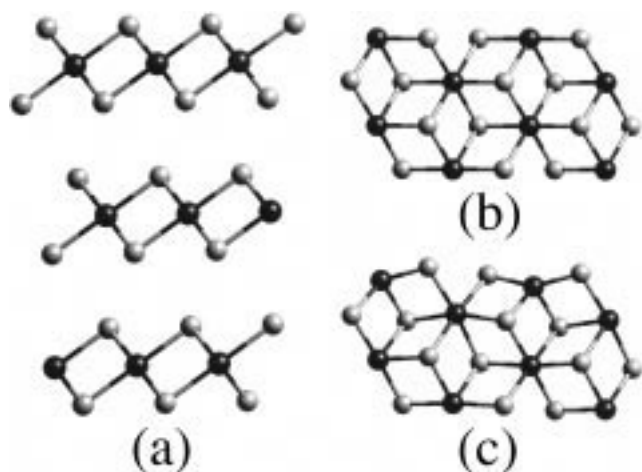(29) Car, R.; Parrinello, M. *Phys. Rev. Lett.* **1985**, *55*, 2471.

2748 *J. Am. Chem. Soc., Vol. 120, No. 12, 1998*

Boero et al.

Figure 2. Ball and stick representation of the $MgCl_2$ layered structure (a), the unrelaxed (110) surface (b), and the same surface after the relaxation (c). Details about the relaxation are given in the text. (Dark gray atoms are Mg, light gray atoms are Cl.)

to the Car−Parrinello lagrangian L^{CP}

$$\mathsf{L}^{CP} \rightarrow \mathsf{L}^{CP} + \lambda_\xi \cdot [\xi(\{\mathbf{R}\}) - \xi_0] \qquad (1)$$

where λ_ξ is the Lagrange multiplier relevant to the constraint $\xi(\{\mathbf{R}\})$ that fixes the reaction path. In the present case, the reaction coordinate is taken to be the distance $|\mathbf{R}_{chain} - \mathbf{R}_{C_2H_4}|$ between one of the carbon atoms of the incoming ethylene ($\mathbf{R}_{C_2H_4}$) and the C belonging to the chain-terminator group or the carbon atom of the chain directly bound to titanium in the case of subsequent insertions ($\mathbf{R}_{chain}$) (details can be understood looking at Figure 8); ξ_0 is the particular fixed value during a CPMD run. During each constrained CPMD run, the system was equilibrated for 1.5 ps. The free energy difference was then computed according to the "Blue Moon" ensemble prescription, which in our particular case reads[45]

$$\Delta F = \int_A^B \mathrm{d}\xi_0 \langle \lambda_\xi \rangle \qquad (2)$$

where A and B stand for the initial and final values of the considered constraint along the reaction path. Free energies in our calculations are affected by an average error bar of 2.2 kcal/mol. Electron localization functions (ELF) relevant to the most important steps of the polymerization have been computed according to refs 46−49. Simulations were performed with the CPMD code.[50]

Results and Discussion

The Active Surface. We started our analysis with bulk $MgCl_2$, whose crystal structure is layered and belongs to the $R\bar{3}m$ space group. A side view of the crystal is shown in Figure 2a. We took the initial geometrical parameters reported in ref 51 and optimized the *a* lattice constant consistently within our functionals. The *c* crystallographic axis was assumed to be equal to the experimental value and not optimized since along

(44) Mülders, T.; Krüger, P.; Swegat, W.; Schlitter, J. *J. Chem. Phys.* **1996**, *104*, 4869.

(45) Sprik, M.; Ciccotti, G. private communication.

(46) Becke, A. D.; Edgecombe, K. E. *J. Chem. Phys.* **1990**, *92*, 5397.

(47) Savin, A.; Becke, A. D.; Flad, J.; Nesper, R.; Preuss, H.; von Schnering, H. G. *Angew. Chem.* **1991**, *103*, 421.

(48) Savin, A.; Flad, H.; Flad, J.; Preuss, H.; von Schnering, H. G. *Angew. Chem.* **1992**, *104*, 185.

(49) Silvi, B.; Savin, A. *Nature* **1994**, *371*, 683.

(50) We have used the code CPMD, version 3.0, developed by J. Hutter, P. Ballone, M. Bernasconi, P. Focher, E. Fois, S. Goedecker, M. Parrinello, M. Tuckerman at MPI für Festkörperforschung and IBM Zurich Research Laboratory (1990−1996).

(51) Experimental crystallographic data after: Dorrepaal, J. *J. Appl. Crystallogr.* **1984**, *17*, 483.
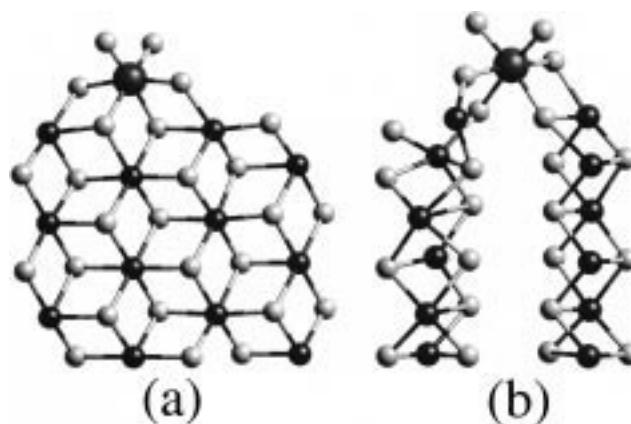

Figure 3. Titanium configurations relevant to the Corradini model (a) and the *bridging* structure (b). Colors are the same as in Figure 1 for the substrate while the Ti is the larger ball clearly visible on the surface.

this direction van der Waals forces, not included in any class of density functionals, play the major role. The resulting optimized bulk value was 3.651 Å, which differs from the reported experimental one (3.640 Å) by about 0.3%. The Mg−Cl bond lengths of the relaxed bulk were 2.520 Å (exp 2.530 Å[52]). We then relaxed a $MgCl_2$ (110) surface cleaved from the bulk. The effects of this relaxation propagate to the bulk atoms up to the third or fourth neighbor. For this reason we chose a thickness of six neighbors. The energy gain of the relaxation was 167.4 kcal/mol. As a consequence of this process, we noticed a tendency of the Cl atoms on the surface to stretch out slightly, while the magnesium atoms tend to pucker partially toward the bulk. The 180° typical bulk angle of Cl−Mg−Cl reduced to 154° on the relaxed surface while the Mg−Cl bond lengths shortened to 2.403 and 2.322 Å. The global effect results in a partial screening of the unsaturated Mg sites on the surface by the surrounding chlorines (see Figure 2b,c).

Ti Active Sites. The first titanium site considered was the model proposed by Corradini and co-workers[24,25] in which a 6-fold Ti sits on the $MgCl_2$ surface in a configuration similar to the bulk magnesium of the substrate. This configuration minimizes the number of unsaturated bonds in the neighborhood of the Ti adduct and seems then to be a realistic candidate for an active site. A full relaxation of the supercell internal structural parameters was performed, attaining the equilibrium geometry shown in Figure 3a. This 6-fold coordinated Ti can be regarded as a substitutional atom replacing a magnesium in the $MgCl_2$ structure. As a matter of fact, even if a coordination number of 6 is possible for titanium, high bond distortions are required for a free tetrahedral $TiCl_4$ molecule coming from gas phase to stick onto the (110) surface in a similar configuration. More likely, these sites can be formed by chemisorption of $TiCl_4$ during the preparation of the substrate.[13]

Alternative models consisting of undercoordinated 5-fold Ti sites have recently been proposed in ref 23. We attempted a relaxation of these configurations and found that they are indeed stable when isolated $TiCl_4$−$MgCl_2$ systems are considered,[53] but when they were placed on a (110) surface and a global relaxation was allowed, the geometries indicated as **a** and **c** in

(52) See, for example: *Gmelins Handbuch der Anorganischen Chemie*; Verlag Chemie GmbH: Weinheim, 1951.

(53) We found the two stable structures of $TiCl_4$−$MgCl_2$ with related equilibrium geometries very close to the ones described in Figure 1 of ref 23. The structure labeled as **b** was energetically lower by 4.4 kcal/mol with respect to **a**. The ordering is the same as in ref 23 where a difference of 7.9 kcal/mol is reported.

Ziegler−Natta Heterogeneous Catalysis

J. Am. Chem. Soc., Vol. 120, No. 12, 1998 2749

Figure 4. The 5-fold Ti configuration obtained by simulation of TiCl$_4$ deposition on a MgCl$_2$ (110) surface as described in the text.

Table 1. Main Geometrical Parameters for the π-Complexes

	corradini	*bridging*	5-fold	2a (C_s)[a]	2a′(C_s)[a]	b
Ti−CH$_3$	2.160	2.167	2.188	2.00	2.00	2.04
Ti−C^1	2.273	2.272	2.876	2.35	2.86	3.05
Ti−C^2	2.249	2.249	2.804	2.86	2.40	3.05
C^1−C^2	1.409	1.407	1.356	1.35	1.35	1.33
∠C^{1}C^{2}Ti	72.8	72.7	79.2	55.5	95.8	77.3

a,b Quantum chemical results are from refs 19 (*a*) and 22 (*b*). Atoms are labeled according to ref 19. Distances are in Å; angles, in deg.

in the previously discussed titanium configurations have to be replaced by methyl groups. In the case of the Corradini configuration, as well as the *bridging* one, we substituted one of the terminal Cl atoms with a CH$_3$ group and removed the other one in order to satisfy the basic requirement of an undercoordinated site. On the other hand, in the case of the 5-fold site only one chlorine must be replaced by a methyl group and no extra atom removal is needed in order to generate a vacant site. To this extent, the activation of this site is less expensive than the previous one. In each case the oxidation state is Ti(IV), according to the recent X-ray absorption results of Jones and Oldman,[10] which indicate Ti(IV) rather than Ti-(III) as the dominant catalytic species. Relaxations of these two activated structures did not display any remarkable geometrical modifications. Only a slight Ti−C bond displacement occurred in the first configuration as a consequence of the double Cl removal.

In the first case, a C$_2$H$_4$ molecule in the vicinity of the Ti site formed a stable π-complex with the equilibrium geometry reported in Table 1. We note that the local geometry of this π-complex is not too different from the all-electron findings of ref 22 in which SCF-MCPF calculations on a sterically similar system is reported. The π-complex formation is an energetically downhill process, and the resulting ethylene coordination energies are about 46.2 kcal/mol according to LDA and 42.1 kcal/mol according to BLYP.

A π-complex with practically the same local geometry was found in the case of the *bridging* configuration (see Table 1). For this reason the insertion process was studied only for the on-layer structures.

Attempts to obtain an analogous complex on the spontaneously formed 5-fold site could not give rise to stable structures at the LDA level but a complete insertion occurred. However calculations within BLYP functional estimated a coordination energy of 45.3 kcal/mol and a small barrier of 6.7 kcal/mol, separating a stable π-complex from the transition state. This is not surprising, since it has already been noticed that very often LDA underestimates insertion barriers.[55−57] A complete discussion of the insertion processes will be given in the next section, but we anticipate that this barrier is significantly lower than the analogous one for the Corradini model, supporting the conclusion of a higher reactivity associated to this titanium configuration. The main geometrical parameters of this π-complex are reported in Table 1.

It is worthy of note that in both cases the resulting coordination energies are close to the quantum chemical results obtained on a CH$_3$TiCl$_2^+$ sterically open cluster.[19]

At this stage we could then identify two different configurations of titanium on the MgCl$_2$ surface which can act as active sites and whose remarkable differences rely essentially on the local bonding environment. To investigate the relevant reactivities we studied the insertion reaction in both cases.

ref 23 relaxed to the 6-fold configuration of the previous model with an energy gain of about 14.0 and 15.7 kcal/mol at the LDA and BLYP level, respectively. This is due to the fact that another nearby chlorine atom, which does not belong to the original TiCl$_4$−MgCl$_2$ structure is involved in the relaxation leading to the formation of the 6-fold Ti site. On the other hand, an attempt at global network relaxation on a structure similar to **b** or **d** of ref 23 gave a surprising *bridging* configuration reported in Figure 3b. The local geometry of this Ti site turned out to be similar to the previous one, with the titanium 6-fold coordinated. The most noticeable differences rely on the more stressed Ti−Cl−Mg bonds with the substrate which became ∼0.1 Å larger than in the Corradini case. This configuration is however 43.1 kcal/mol higher in energy than the 6-fold on-layer Ti configuration and thus seems energetically unfavorable. These results underscore the need to take into account all the surrounding atoms of the active surface where the titanium site is located in geometry optimizations.

For this reason, without making any model assumption, we allowed a TiCl$_4$ molecule to deposit freely on the MgCl$_2$ surface. We observed that in about 1.0 ps the molecule binds to the surface in a 5-fold configuration not too different from the support models **b** and **d** of Puhakka et al. This configuration is dynamically stable and only 8.1 kcal/mol higher in energy than the 6-fold on-layer configuration. The spontaneous formation of such a site and its stability, even in comparison with the Corradini model, makes this support a good alternative candidate as a catalytic active center. We observe that this site locally minimizes the number of defects of the surface, restoring the 6-fold and the 3-fold coordinations on a Mg and a Cl atom, respectively. The geometry of this site is shown in Figure 4.

These results were checked carefully within the BLYP approach. Our findings indicate that in this case the two sites, i.e., the 5-fold configuration and Corradini's one are stable configurations separated by 10.9 kcal/mol, the 6-fold structure being the lower minimum, in perfect agreement with the LDA results. This energy difference between the 5-fold and the 6-fold Ti can be ascribed to the fact that the former structure has one bond less than the latter.

π-Complex Formation. Prior to the alkene insertion, complexes of metal−alkene form. Since both these processes occur when a titanium−carbon bond exists,[54] the titanium sites have to be activated in some way. Experimentally active centers are created by introducing AlEt$_3$ in the reaction chamber in order to remove Cl atoms bound to Ti and to promote alkylation of titanium.[7,11] To simulate these active centers, chlorine atoms

(54) Eisch, J. J.; Piotrowski, A. M.; Brownstein, S. K.; Gabe, E. J.; Lee F. L. *J. Am. Chem. Soc.* **1985**, *107*, 7219 and references therein.

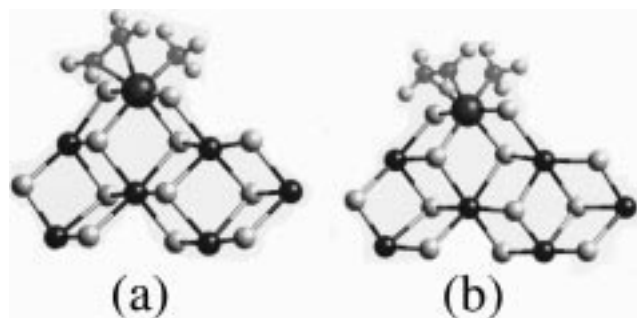(55) Meier, R. J.; van Doremaele G. H. J.; Iarlori, S.; Buda, F. *J. Am. Chem. Soc.* **1994**, *116*, 7274.
(56) Margl, P.; Ziegler, T. *J. Am. Chem. Soc.* **1996**, *118*, 7337.
(57) Deng, L.; Margl, P.; Ziegler, T. *J. Am. Chem. Soc.* **1997**, *119*, 1094.

Figure 5. Two possible configurations of the π-complex in the case of the activated Corradini center. During the dynamics the system can switch from a to b. Only the portion of the system around the catalyst is shown, not the whole supercell. The small light-gray atoms around Ti are the C of the ethylene (on the left) and of the CH_3 (on the right) carrying their H atoms (small white balls).

Table 2. Activation Barriers and Energetics of the Product with Respect to the π-Complex[a]

	Corradini	5-fold (1)	5-fold (2)	ref 19	ref 22	exp
activation barrier	14.9	6.7	6.1	4.3	0.9	6−12
product	−5.8	−23.3	−10.5	−11.1	−23.6	−22.2

[a] We report only the BLYP total energy estimation to compare with literature data. Free energies, LDA total energies and experimental references are quoted in the text and shown in Figure 5. In our 5-fold simulations (1) refers to the first insertion and (2) to the chain propagation. References 19 and 22 report only the first insertion. In the table only the best estimates of refs 19 and 22 are reported.

Ethylene Insertion Processes. A free molecular dynamics trajectory (1.6 ps) of the π-complex obtained from the Corradini configuration displayed a switching between two possible orientations of the coordinated ethylene molecule. Roughly speaking the two configurations differ in the orientation of the ethylene carbon double bond, which can be either parallel or orthogonal to the Ti−CH$_3$ axis as shown in Figure 5. Both of these configurations are characterized by the same average energy and the switching observed indicates that little or no barrier exists between them. No spontaneous insertion of C_2H_4 occurred, stressing the fact that a barrier has to be overcome to give rise to the polymerization. To estimate this barrier, we performed a constrained dynamics at 323 K and applied the method of the average constraint force to compute the free-energy profile.

We found that a barrier of 12.7 kcal/mol separates the π-complex from the transition state and that the former was a local minimum of the energy surface at LDA level. Further calculations using the BLYP functional located this energy difference at 14.8 kcal/mol, substantially confirming the LDA results. These results compare well with quantum chemical results of ref 19 on a Ti(III)-based catalyst and with available experimental data, which span in time from the original work of Natta himself[58] (10 kcal/mol) to more recent ones[59,7] that estimate barrier values ranging between 6 and 12 kcal/mol (see Table 2) according to the different experimental conditions and systems considered. In Figure 6 the free energy and the total energy differences are plotted as a function of the reaction coordinate, i.e., the intercarbon distance between the incoming ethylene and the CH$_3$ group as described in section II. The depicted reaction pathway passes through a four-membered ring structure[17] before sliding down to the complete chain formation.

(58) Natta, G.; Pasquon, I. *Adv. Catal.* **1959**, *11*, 1.
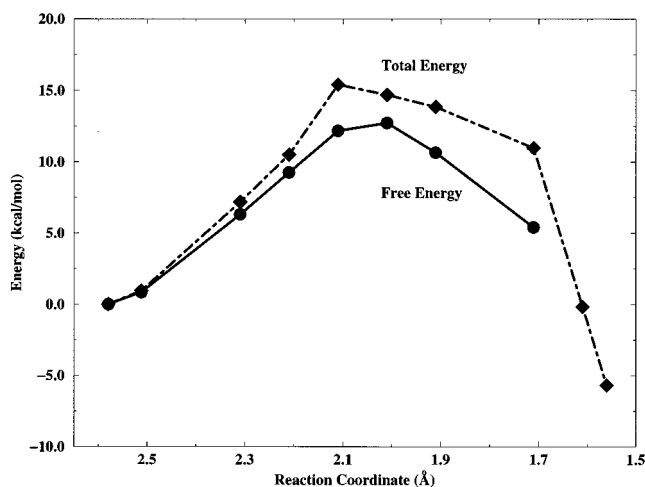(59) Machon, J.; Hermant, R.; Hoteaux, J. P. *J. Polym. Sci. Symp.* **1975**, *52*, 107.

Figure 6. Free energy profile of the ethylene insertion the case of the Corradini site as obtained from constrained CPMD (filled circles). The corresponding average total energy is reported for matter of comparison (filled diamonds). The solid and dot−dashed lines are intended only as a guideline to eye. The reaction coordinate axis ranges from the π-complex to the insertion going from left to right. The free energy curve does not follow the total energy profile because large fluctuations of the constraint affected the last two points in which the reaction coordinate is no longer a simple atom−atom distance, but reorientation and displacement of the polymer chain play the major role.

We noticed that during the insertion process the distance between the Ti and one of the H atoms of the methyl group reduced to 1.912 Å[3] from its initial value of 2.468 Å[3] as a consequence of the tilt of the CH$_3$ group. This is a clear signature of an agostic interaction occurring between Ti and H, the effect of which is to reduce the steric hindrance with the approaching alkene. We observed a bond weakening of the Ti with a Cl of the substrate during the ethylene coordination and insertion phases of the same type reported by Jensen et al.[22] Surprisingly, only a small energy gain was found in this case between the reactant (π-complex) and the product (insertion), namely less than 6 kcal/mol (5.8 kcal/mol according to BLYP results). This estimate is lower than the most accurate quantum chemical calculations in isolated clusters ($\Delta H = 21.6$ kcal/mol and $\Delta E = 23.6$ in ref 22 and $\Delta E = 11.10$ kcal/mol in ref 19), which however depend markedly on the considered system, the level of the theory and the basis set used. Experimental overall reaction enthalpy estimations for ethylene insertion give 22.2 kcal/mol.[61] This might point to a marginal role of the Corradini center in the actual polymerization process. The details of the energetics are summarized in Table 2 and Figure 6.

In the case of the 5-fold site a complete insertion has a much lower activation barrier (6.7 kcal/mol at BLYP level) as shown in Figure 7. This is due to the fact that one of the Cl atoms bound to Ti has no bond with the substrate and can easily displace, allowing the alkene to approach as can be easily understood by looking at Figure 8. Furthermore, the fact that the Ti site has only three bonds with the substrate gives additional degrees of freedom to this configuration. Such a flexibility does not exist in the case of the Corradini model where all the Cl atoms bonded to Ti are shared with the underlying substrate. Analogous to the previous case, we observed that the ethylene insertion proceeds via agostic interaction with a methyl group tilting and a shortening of the Ti−H distance from 2.627 to 1.959 Å. As in the previous case,

(60) Chien, J. C. W. *J. Am. Chem. Soc.* **1959**, *81*, 86.
(61) Aylward, G. H.; Findlay, T. J. V. *SI Chemical Data*, 2nd ed.; John Wiley and Sons: Hong Kong, 1985.
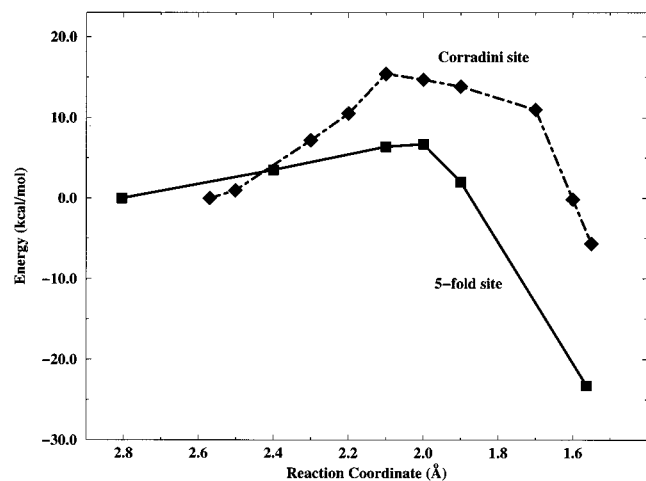
Ziegler−Natta Heterogeneous Catalysis

J. Am. Chem. Soc., Vol. 120, No. 12, 1998 2751

Figure 7. Comparison of the energetics relevant to the Corradini site and the 5-fold one from the π-complex (left) to the complete insertion (right). In both cases the π-complex was assumed as reference energy (see text for details).
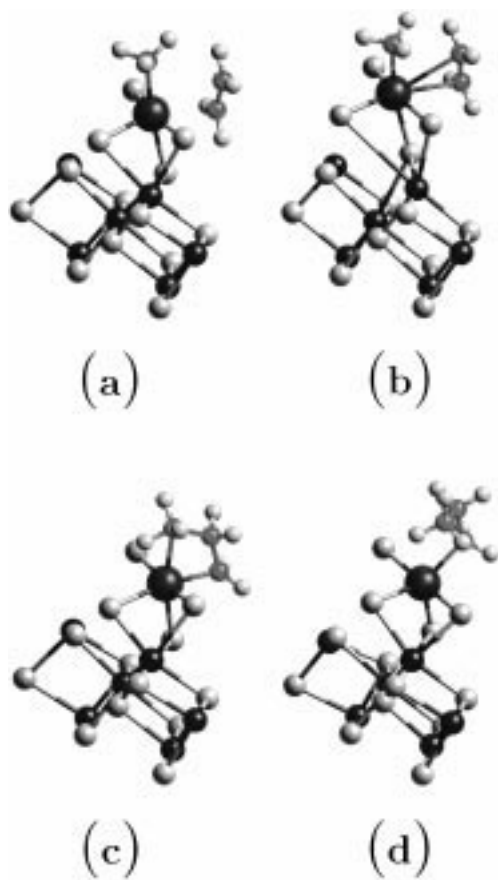

Figure 8. Snapshots of the most important steps in the insertion reaction for the 5-fold Ti site: the ethylene approaching (a), the π-complex formation (b), the transition state (c), and the formed chain after the turning off of the agostic interaction (d).

Figure 9. ELFs of the most important steps in the insertion reaction for the 5-fold Ti site. They refer to the π-complex (a), the transition state (b), and the product after the chain displacement and the switch-off of the agostic interaction (c). In each case the slice for the projected ELF is defined by the plane containing the two ethylene C atoms and the Ti. In a and b the C of the methyl group is practically coplanar, while in c it lies out of the projection plane, toward the reader. Numerical values of the ELF's range across the spectrum from ELF $=$ 0 (blue) to ELF $= 1$ (red). The purple atom at the center of the figure is Ti, while gray atoms are C, white H, green Cl and the pink ones, in the lower part of the figures, the Mg of the substrate.

a weakening of the Ti bond with the substrate occurred during the reaction. Experimental evidence for a metal−H−C agostic structure has been reported by Schmidt and Brookhart[62] on ethylene hydride complexes. Even if, as pointed out by the same authors, their results do not rule out other alternative reaction pathways, the agostic-assisted insertion is still the simplest and most reasonable mechanism for metallocene catalysts. In Figure 9 the ELFs relevant to the π-complex (a),
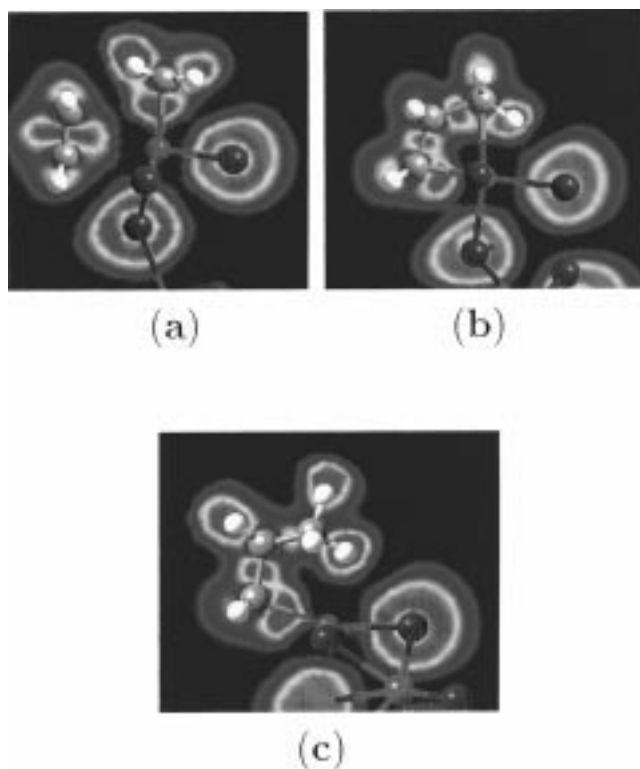
the transition state (b), and the final product (c) are reported. The regions of strong localization are identified by the red areas. The cleavage of the Ti−CH$_3$ bond and the formation of the new ones, CH$_3$−CH$_2$ and Ti−CH$_2$, are clearly visible going from a to c: a charge delocalization occurs in the former case, while high localization domains arise in the latter.

An unconstrained dynamics after the insertion has shown that the CH$_3$−CH$_2$−CH$_2$ chain is easily displaced far from the catalyst, leaving the Ti sufficiently unscreened to allow further alkenes to approach. This displacement occurred together with a rotation of the methyl group, which turns off the agostic interaction. The energy gain from the π-complex to the product in this case amounts to 23.3 kcal/mol (see Table 2 and Figure 7).

As a further step we studied the insertion of a second ethylene in the case of the 5-fold site in order to understand the chain propagation process and to work out the energetics relevant to subsequent insertions for which, to the best of our knowledge, no calculation have so far been attempted. In our search for possible directions from which an incoming ethylene could approach the catalyst, we found that if the alkene was introduced from the right side of the chain, referring to Figure 8d, the strong steric repulsion from the chain prevents any stable complex formation. On the contrary, in the case of insertion from the left side, where the Ti center is unshielded, a large amount of empty space exists, allowing a nearby ethylene to approach the catalyst and to form a stable π-complex. This occurs with a

(62) Schmidt, G. F.; Brookhart, M. *J. Am. Chem. Soc.* **1985**, *107*, 1443.
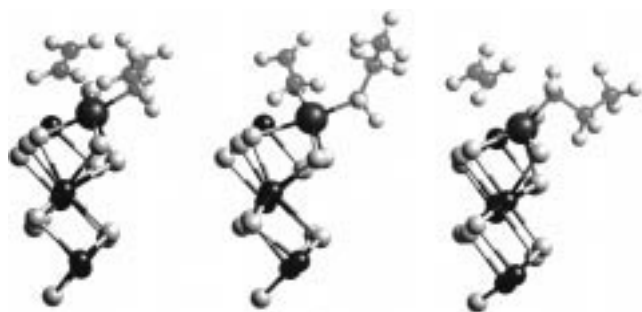
Figure 10. Reorientation of the alkyl chain during the approach of the second ethylene and formation of the π-complex as obtained by free dynamics. The snapshots are time ordered from the left to the right.

large displacement of the chain which roughly speaking orients parallel to the surface of the support from the side opposite to the ethylene incoming direction (see Figure 10 for details). This new dynamical equilibrium structure corresponds to an energy gain of 33.4 kcal/mol. The stereochemistry of the alkyl chain results as a consequence of the self-arrangement of the CH_2 groups along the chain itself occurring in the π-complex formation phase. We found that the formation of such a complex occurred with a switching of the interaction between Ti and hydrogen in a way very similar to the γ- to β-agostic transition observed in homogeneous catalysis:[63] the CH_3 group in the equilibrated geometry is far from the titanium and agostic interaction occurs between Ti and a hydrogen of a nearby methylene unit along the polymer. As well as in the case of the first insertion, there are two possible orientations of the carbon double bond of the ethylene: orthogonal and parallel to the $Ti-CH_2$ bond. Even in this case the system can switch between the two during the dynamics. The insertion of the new olefin from this point proceeds very smoothly with an activation energy of about 6.1 kcal/mol (BLYP estimation) and even in this case turns out to be agostic-assisted. The main differences with respect to the chain initiation rely on the fact that now the agostic interaction does not occur between the titanium and one of the hydrogen atoms of the CH_2 group directly bound to it, but with the next methylene along the chain. Even in this case a four-membered ring is the transition state and the $Ti-C$ bond cleavage and formation can be easily understood by looking at Figure 11.

After the insertion of the new alkene, a $Ti-CH_2$ bond shifting takes place in such a way that the equilibrium structure has again a $Ti-C$ bond pointing approximately in the same direction as the original one prior to the addition of the olefin. This allows further ethylenes to approach the catalyst always from the same side and to propagate the chain according to the reaction mechanism just depicted.

(63) Woo, T. K.; Margl, P.; Lohrenz, J. C. W.; Blöchl, P. E.; Ziegler, T. *J. Am. Chem. Soc.* **1996**, *118*, 13021.
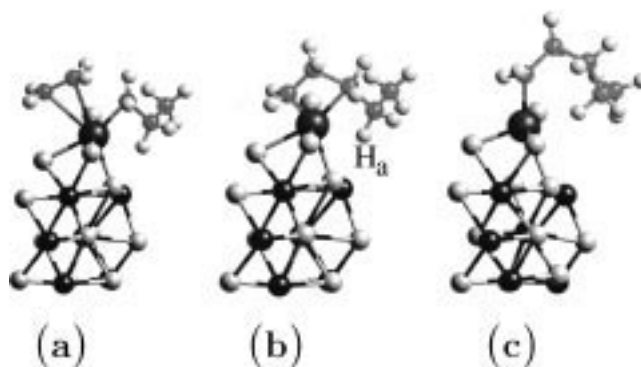

Figure 11. The main phases of the second insertion leading to the chain propagation: the π-complex (a), the transition state (b) and the insertion (c). In b the label H_a indicates the H atom involved in the agostic interaction.

Conclusions

We presented a first principles molecular dynamics study of Ziegler−Natta heterogeneous catalysis at finite temperature, the catalyst being Ti supported on $MgCl_2$, and focused on ethylene polymerization. Our analysis elucidates the energetics relevant to the 6-fold active site of Ti on the (110) surface of the support according to the model proposed in the literature by Corradini and co-workers; in addition, we suggest a possible alternative center consisting of a 5-fold titanium site. The unbiased approach adopted for its formation from gas-phase deposition makes this configuration a suitable candidate as an active site. Its higher reactivity with respect to the 6-fold structure is stressed by the lower activation barrier and the larger overall energy. A rather good agreement concerning the energetics of the process was found with previous quantum chemical calculations and available experimental data.

Our investigation also provides support for the agostic-assisted insertion of alkenes in the Ti−C bond depicting a realistic pathway for the polymerization both in the initial stage and in the chain propagation phase. In this way we address the problem of the reaction mechanism and offer a comprehensive insight into the fundamental problems of this class of catalytic reactions.